*Journal of Thermal Analysis, Vol. 46 (1996) 1061-1079*

Dedicated to Professor Bernhard Wunderlich on the occasion of his 65th birthday

# PHASE STRUCTURE AND VISCOELASTIC PROPERTIES Polypropylene–polystyrene systems with various dispersion of PS component

*M. Pluta, J. Morawiec, M. Kryszewski and T. Kowalewski**

Center of Molecular and Macromolecular Studies, Polish Academy of Sciences
Sienkiewicza 112, 90–363 Łódź, Poland
*Washington University, Department of Chemistry, St. Louis, Missouri, 63130–4899 USA

## Abstract

The phase structure and dynamic mechanical properties of three polypropylene/polystyrene (PP/PS) systems of similar composition but various dispersion of the minor PS component have been examined. Two different PP/PS systems were prepared by polymerization of styrene (ST) molecularly dispersed in PP matrices (with the same initial structure) under the conditions leading to a linear or crosslinked PS component. The third PP/PS system has been prepared blending the homopolymers in the molten state. Studies of materials containing *in situ* polymerized PS revealed nanoscale phase separation of PS (atomic force microscopy) and pointed to the presence of physical entanglements between PS and non-crystalline phase of PP (DSC, dynamic mechanical analysis). The PS component in material prepared by melt mixing appeared to be completely phase-separated into micron-sized domains. Dynamic mechanical analysis revealed also the dependence of viscoelastic behavior of the PP/PS systems on dispersion of the PS inclusions and on the nature of the interface.

**Keywords:** atomic force microscopy, composites, dispersion, phase structure, polymerization *in situ*, polypropylene, polystyrene, viscoelastic properties

## Introduction

In recent years, there has been increasing interest in multicomponent polymer systems. This results from both the practical importance of such systems and from the scientific point of view.

From the structure – physical properties point of view, an interesting two-component polymer system can be obtained by polymerizing a monomer inside a semicrystalline polymer matrix. Previously, we have applied this method to prepare two-component polymer systems in which the styrene monomer (ST) was polymerized *in situ* in the matrices of low density polyethylene (PE) or isotactic polypropylene (PP). We have demonstrated that immiscible systems

*0368–4466/96/ $ 5.00*

*John Wiley & Sons, Limited*
*Chichester*

obtained in this way (PE/PS and PP/PS), are characterized by a specific dispersion of the PS inclusions and that the structure of the semicrystalline polymer matrices is modified to some extent [1–3]. The materials obtained in this way exhibited some interesting changes of physical properties compared to those found for the pure polymer matrix. These included permeability to organic solvents and viscoelastic behavior in PE/PS systems [4, 5], and viscoelastic properties and shrinkage phenomena in PP/PS systems based on oriented PP matrices [6].

The present paper considers the phase structure of a series of PP/PS systems having similar composition but exhibiting various dispersion of the PS constituent, resulting from different preparation methods. The PP/PS systems investigated were obtained by: (i) polymerization of ST inside the PP matrix, (ii) polymerization and crosslinking of ST inside the PP matrix, (iii) melt blending of the homopolymers. Information from structural studies is correlated with the results of dynamic mechanical measurements. The changes of the structure of PP matrices induced by preparation of the PP/PS systems are considered as well.

## Sample preparation

The starting polymer matrices were prepared in the form of films (approximately 0.2 mm thick) from commercial-grade isotactic polypropylene PP F401 (Polish product) as described in [2]. Crystallization was carried out at a relatively low temperature, 298 K, for 30 min, in order to assure a fine spherulitic morphology of the PP matrices.

Two kinds of PP/PS systems were prepared by *in situ* polymerization of ST. In one case the PP films were immersed in the 95:5 (by weight) mixture of styrene monomer and benzoin isobutyl ether (photoinitiator). In the second case the mixture in which PP films were immersed contained in addition 2.5 wt.% of divinylbenzene (DVB) (crosslinking agent). The ST and DVB were purified by distillation. The PP sample was swollen for 1 h at the temperature at which the sample was crystallized (298 K) in order to minimize structure reorganization [7]. The swollen sample was then gently wiped with a blotting-paper and placed between quartz plates of a thermostated chamber. The polymerization of ST was initiated by irradiating both sides of the film for 3 hours with UV light (AS 700 mercury lamps – Austria) at 333 K.

This polymerization condition led to degrees of conversion of ST monomer into PS close to unity [2]. The resulting samples, designated respectively as PP/PS(L) (PS(L) – linear component) and PP/PS(C) (PS(C) – crosslinked component), were carefully rinsed in toluene and vacuum-dried at 333 K for 2 weeks. The weight loss in the course of this treatment was found to be about 0.2–0.3%. The final PS content ($m_{PS}$) calculated from the expression

$((m_{PP/PS}-m_{PP})/m_{PP})^{*}100\%$ is given in Table 1 ($m$ – denotes the mass of the respective sample).

**Table 1** Polypropylene/polystyrene systems characteristics

| Sample | PS contents, $m_{PS}$ / % | Preparation | PS structure |
|---|---|---|---|
| PP/PS(L) | 13.7 | *in situ* synthesis | linear |
| PP/PS(C) | 13.3 | *in situ* synthesis | crosslinked |
| PP/PS-M | 14.0 | melt blending | linear |

For comparison small PS(L) and PS(C) samples were prepared at conditions as described above. The PS(C) sample was not soluble in toluene, indicating high degree of crosslinking.

A third two-component system composed of the PP and atactic polystyrene (PS BDH Chemicals, Ltd., Poole England) was prepared by melt mixing (473 K) in three passes through a Brabender single-screw extruder. The blend was then used for preparation of a sample of a composition comparable to the two previous systems, denoted as PP/PS-M (Table 1). The compression molding and crystallization conditions were identical to those used in the preparation of starting PP matrix films.

Prior to further studies all samples were annealed at 333 K in order to make their thermal histories similar.

## Sample characterization

Differential scanning calorimetry (DSC) curves were obtained using a DuPont 2000 TA calorimeter at a heating rate of 10°C $min^{-1}$. The glass transition temperature for the polystyrene samples was determined as the temperature of the inflection point on the curves describing the heat capacity changes. The heat of fusion and the melting temperature of the PP were determined as well.

Observations of the supermolecular structure and determination of the size of polystyrene inclusions in PP matrices were carried out using light microscopy (LM), on thin sections (2.5 μm) microtomed at 293 K (Tesla BS 490A ultramicrotome).

Observations by atomic force microscopy (AFM) were performed with the aid of a Nanoscope III-M system (Digital Instruments) working in the non-invasive 'tapping mode' [8]. D-type piezoelectric scanners (scan range 15 μm×15 μm) and 120 μm silicon cantilevers with mechanical resonance frequencies in the range of 300 kHz, designed specially for tapping mode, were used throughout the study. In order to minimize the probe-tip – sample interactions, the cantilever oscillation amplitude was kept below ±10 nm, typical set-points were in the range of 80–90% of free oscillation amplitude. Scan frequencies were in the range from 2–10 Hz, depending on the scan size. Some images were low-pass filtered, in order to suppress the high-frequency noise.

Careful checks indicated that features of interest were not distorted by filtering. Whenever necessary, artificial light shadowing was applied, in order to facilitate simultaneous visualization of surface features in the large height range.

Gel permeation chromatography (GPC) of polystyrene materials (PS(L), PS) was performed employing an LKB 2150 HPLC pump, a set of Toyo Soda G4000HXL and G2000HXL columns, and IR detector. THF was used as an eluent with a flow rate of 0.8 ml $min^{-1}$, the chromatograms were analyzed according to calibration on TSK standard PS.

The mechanical properties were measured with a Rheometrics Mechanical Spectrometer Model 800. The shear storage modulus ($G'$) and loss tangent (tan $\delta$) of the samples were obtained as a function of temperature at a constant frequency of 5 rad $s^{-1}$ and at a heating rate of 2.5°C $min^{-1}$. The tested samples had the form of 20 mm×10 mm strips.

## Results and discussion

### *Characteristics of polystyrene samples*

Molecular characteristics of the PS(L) and PS samples are listed in Table 2. The data from this Table indicate that the polystyrene obtained by UV-initiated polymerization (PS(L) sample) is characterized by lower molecular weight ($M_n$) and higher polydispersity index ($M_w/M_n$) compared to the PS sample.

**Table 2** Molecular characteristics of polystyrene samples

| Sample | $M_n$ | $M_w/M_n$ |
|---|---|---|
| PS(L) | 5880 | 6.02 |
| PS | 107000 | 2.78 |

### *Differential scanning calorimetry*

Figure 1 presents the DSC curves of the plain polypropylene sample, two-component polypropylene/polystyrene systems as well as those of polystyrene samples.

The DSC curves of the polystyrene samples clearly show the glass transition effect. The glass transition temperature ($T_g^{PS}$) in photopolymerized samples, PS(L) and PS(C), is lower by about 20 K than the glass transition temperature of plain PS (Table 3). This difference is related to various molecular weight characteristics ($M_n$, $M_w/M_n$) of PS in these samples.

The plain PP sample and the PP component in the PP/PS-M system both exhibit a weak endotherm at lower temperature range, with an onset at about 310 K. This endotherm reflects the melting process of the less stable smectic phase of PP, present in both samples as they were prepared by crystallization from the melt at relatively large supercooling ($\Delta T$=448 K) followed by an annealing process at 333 K. In our previous studies [2] we have established that

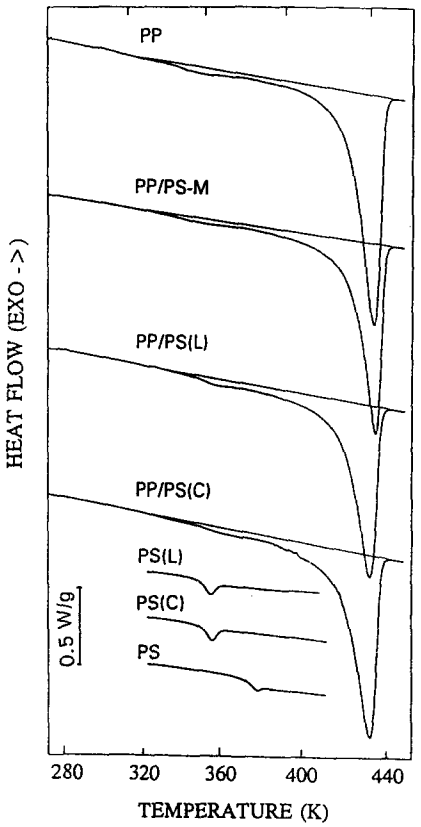


**Fig. 1** DSC curves of PP sample, PP/PS systems and polystyrene materials

swelling of the PP matrix with ST facilitates transformation of the smectic phase to the more thermodynamically stable, monoclinic phase. However, under the sample preparation conditions equivalent to those used in the present work, this transformation was never complete. Thus the smectic phase is also present in the PP component of the PP/PS(L) and PP/PS(C) systems. In these systems, however, it exhibits enhanced thermal stability – the corresponding endotherm appears at a higher temperature range (with an onset at 340 K), coinciding with the glass transition of the PS(L) and PS(C) components. For this reason the heats of melting of the smectic phase and the values of $T_g^{PS}$ for the respective components of considered systems were not evaluated.

The strong endothermal effect observed near 433 K for the plain PP and polypropylene/polystyrene samples is related to the melting process of the PP crystalline phase. The heats of fusion of the polypropylene phase ($\Delta H_m^{PP}$) were calculated by integration of a melting peak, their values were normalized to the mass of PP and were used to calculate the degree of crystallinity of PP ($X_c$). (The heat of fusion of a 100% crystalline PP was assumed to be 209 J $g^{-1}$ after

[9].) The obtained results and the values of the temperatures of the onset of melting ($T_o^{PP}$) and the melting peak ($T_m^{PP}$) are gathered in Table 3. It can be seen from Table 3 that $X^{PP}$, $T_o^{PP}$ and $T_m^{PP}$ for the PP in the PP/PS(L) and PP/PS(C) systems are comparable to or somewhat lower than those parameters determined for the plain PP sample. This indicates that swelling with the styrene monomer and its subsequent polymerization inside the PP matrix lead to some decrease of the overall crystallinity of the PP crystalline phase and – as it was mentioned above – to an enhancement of thermal stability of the smectic phase. We believe that these effects are caused by [2]: (i) more defective nature of PP crystallites formed upon swelling-induced crystallization (SIC); (ii) incorporation of PS inclusions into the noncrystalline and smectic phase regions of PP and into the surface layers of PP crystallites.

The calorimetric parameters of the PP phase of the PP/PS-M system are close to those for the plain PP sample. This implies that the PS inclusions did not affect the crystallization process of PP during preparation of the PP/PS-M blend.

**Table 3** DSC melting data and crystallinity degree for plain PP sample, PP components in polypropylene/polystyrene systems and the glass transition temperature for pure polystyrene samples

| Sample | $\Delta H_m^{PP}$/J g$^{-1}$ | $T_o^{PP}$/K | $T_m^{PP}$/K | $X_c$/% | $T_g^{PS}$/K |
|---|---|---|---|---|---|
| PP | 88.3 | 424.5 | 435.9 | 42.2 | – |
| PP/PS(L) | 83.1 | 420.7 | 433.4 | 39.7 | a |
| PP/PS(C) | 84.2 | 419.7 | 433.2 | 40.2 | a |
| PP/PS-M | 89.6 | 423.8 | 435.5 | 42.9 | a |
| PS(L) | – | – | – | – | 353.1 |
| PS(C) | – | – | – | – | 354.7 |
| PS | – | – | – | – | 376.6 |

*a*: not evaluated

$\Delta H_m^{PP}$ – heat of fusion of PP crystalline phase, $T_o^{PP}$ – temperature of melting onset of PP, $T_m^{PP}$ – temperature of melting peak of PP, $T_g^{PS}$ – glass transition temperature of the pure TS materials.

## *Light microscopy*

The differences of the phase structure of PP/PS(L), PP/PS(C), PP/PS-M and PP are illustrated in the micrographs of thin sections presented respectively in Figs 2a–d. Various sizes and distribution of PS inclusions within the individual PP/PS systems can be distinguished. The PP/PS-M sample (components mixed in the molten state) exhibits a typical morphology of immiscible polymers (Fig. 2c) [10]. The PS component in this system consists of droplet-like and extended domains with sizes ranging from 1 to 20 μm.

The micrographs of the PP/PS(L) and PP/PS(C) systems (Fig. 2a and 2b) indicate that the dispersion of the guest polymer is much greater than in the

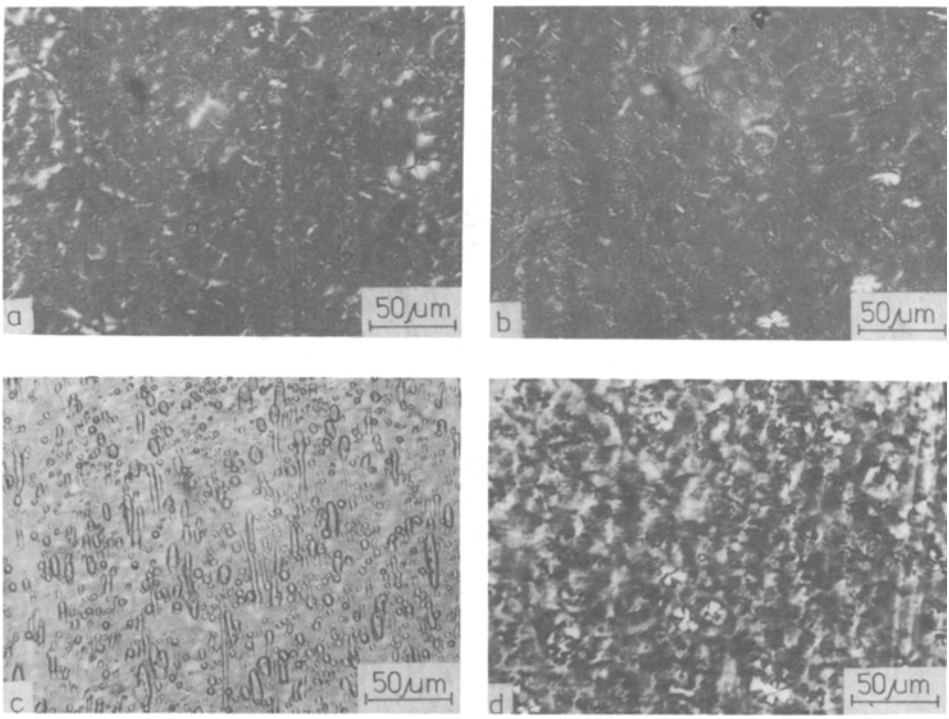


**Fig. 2** Light microscopy micrographs obtained at crossed polarizers for sections of the following samples: a) PP/PS(L), b) PP/PS(C), c) PP/PS-M, d) PP

PP/PS-M sample. The higher dispersion of PS in the systems in which the second component (PS) was polymerized *in situ* results from the high dispersion of its precursor (ST), which during swelling process was able to penetrate into the intraspherulitic, interlamellar regions of PP. These results indicate that only the fraction of PS accumulated in the interspherulitic regions, formed the domains large enough to be identified on light micrographs. Such domains are less readily discernible on the micrograph of the sample containing crosslinked PS (compare Fig. 2a and 2b). It has to be pointed out that the differences in PS content in the PP/PS(L) and PP/PS(C) systems (Table 1), are too small to account for the observed differences of the phase structure. We rather propose that these differences reflect the fact that due to the decrease of its mobility upon crosslinking, *in situ* polymerized PS has been more effectively trapped in the intraspherulitic regions of PP matrix of PP/PS(C) systems.

The supermolecular organization of polypropylene in the plain PP sample and in PP matrices containing polystyrene inclusions seems to be similar. It exhibits a spherulitic morphology with the average spherulite diameter of 10 to 20 μm.

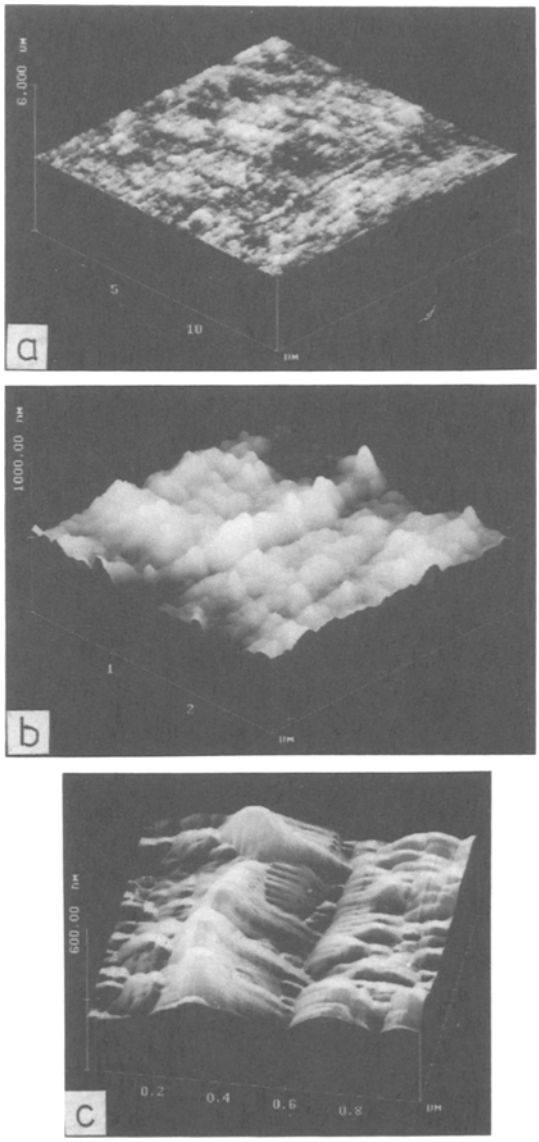


**Fig. 3** 3-D renditions of tapping-mode AFM topographs of the surface of plain PP exposed by brittle fracture at liquid nitrogen temperature. Scan ranges: a) 15 μm×15 μm; b) 3 μm×3 μm; c) 1 μm×1 μm.
Vertical scale coding: a) and b) – grey scale; c) artificial illumination. The image shown in Fig. 3c was low-pass filtered in order to suppress the residual high-frequency noise

## *Atomic Force Microscopy*

The nanoscale resolution morphology of investigated samples was studied with the aid of tapping-mode AFM. Surfaces for the AFM studies were exposed by brittle fracture at liquid nitrogen temperature and by room-temperature ultramicrotomy.

### *Brittle fracture surfaces*

Figures 3a–c show fracture surface of the plain PP sample at various scan ranges. The AFM topographs reveal characteristic protrusions with lateral dimensions of the order of 50 nm. Occasionally they have a highly elongated form and are arranged in a semi-periodic manner (Fig. 3c). Based on this observation we interpret these features as bundles of polypropylene lamellae exposed by fracture proceeding along the inter-spherulitic boundaries. The appearance of lamellar bundles exposed in this way depends on the angle between the spherulite radius and the inter-spherulitic boundary. When this angle is closer to 90 degrees (lamellae are viewed end-on) they appear as rounded bumps (Fig. 3b). At smaller angles edges of lamellar stacks get eventually exposed, giving rise to features shown in Fig. 3c.

Fracture surfaces of PP/PS-M sample were very different from those of plain polypropylene. They were highly irregular, with steps up to several micrometers tall occurring every few micrometers. Due to the limited vertical range of our AFM scanner this posed special challenge during imaging. The most prominent features in the relatively flat regions between the steps were partially exposed spherical inclusions of polystyrene. The diameter of the smallest inclusions, like one shown in Fig. 4a, was in the range of 1 μm. The exposed surfaces of PS inclusions were typically very smooth (Fig. 4a–b), which indicates poor adhesion across the polypropylene – polystyrene interface. Areas of polypropylene matrix surrounding the inclusions did not exhibit the well defined features associated in plain polymer with ends and edges of lamellae. This very different topography reflects the different fracture mode of the blend. Due to poor adhesion between the components it is energetically attractive for the fracture pathway to follow the weakest regions at the polymer-polymer interface.

In contrast with physical blends, fracture surfaces of samples containing *in situ* polymerized PS (PP/PS(L), PP/PS(C)) were less distinguishable from those of plain polypropylene applying the tapping mode AFM. In few occasions however, we have found areas in which the features corresponding to lamellae were not well defined (probably due to the fact that fracture path proceeded through the interior of the spherulite). In such areas we have always observed partially exposed spherical inclusions with the diameters of the order of 50 nm (Fig. 5a–c, Fig. 6b–c). Surface of inclusions of cross-linked polystyrene appeared rougher which might suggest stronger interfacial contacts. The significance of observations of nanoscale phase separation in the samples con-

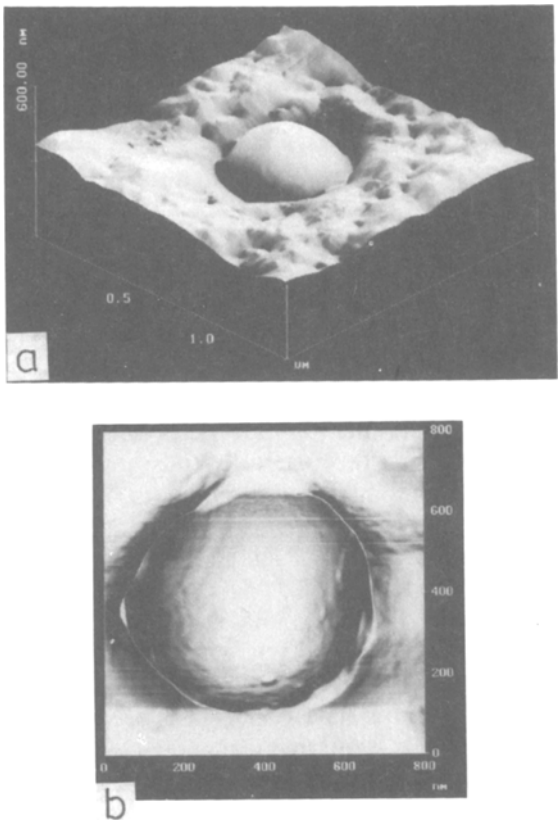


**Fig. 4** Tapping-mode AFM topographs of the surface of PP/PS-M exposed by brittle fracture at liquid nitrogen temperature: a) 3-D rendition of 1.5 μm×1.5 μm scan area containing partially exposed PS inclusion (vertical scale coding – grey scale); b) top-view of the surface of PS inclusion imaged in 800 nm×800 nm scan. The image was low-pass filtered in order to suppress the residual high-frequency noise, vertical artificial light source was applied to enhance the visualization of the surface roughness of the inclusion

taining *in situ* polymerized polystyrene remains unclear due to their sporadic nature. It cannot be ruled out, however, that they are fully representative, and the rarity of their occurrence is caused by the fact that fracture of those samples proceeded preferentially along the inter-spherulitic boundaries.

## Microtomed surfaces

In order to compare the phase structure of the studied samples we have also attempted to expose the bulk of materials by microtoming. The direct comparison of morphologies turned out to be impossible due to reorganization of ex-

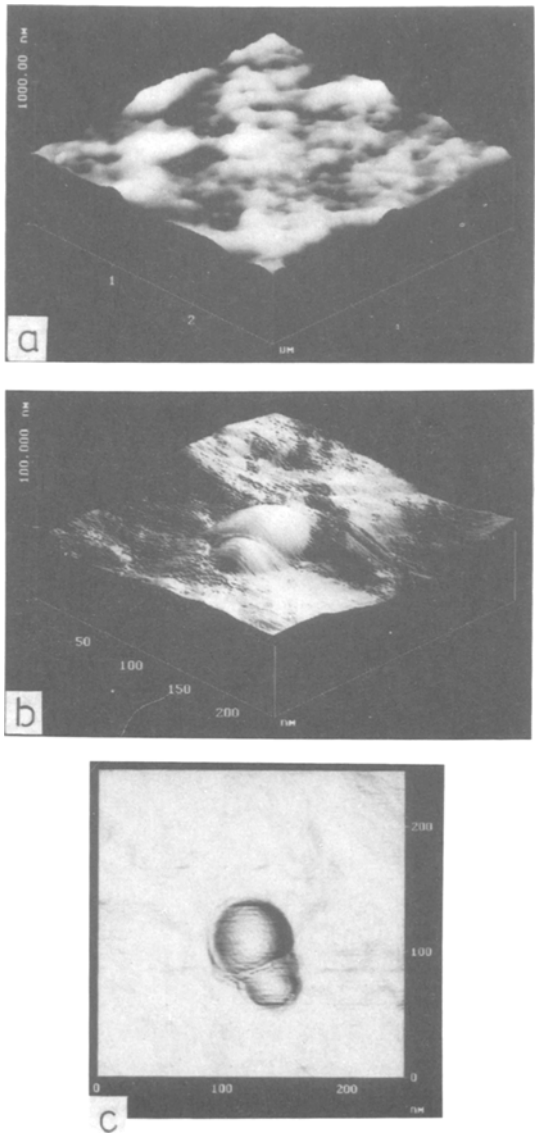


**Fig. 5** Tapping-mode AFM topographs of the surface of PP/PS(L) exposed by brittle fracture at liquid nitrogen temperature: a) 3-D rendition of 3 μm×3 μm scan area (vertical scale coding – grey scale); b) 3-D rendition of the 250 nm×250 nm scan showing partially-exposed nanoscale PS inclusions (vertical scale coding – artificial illumination); c) top-view of the area from b), vertical artificial light source was applied to enhance the visualization of the surface roughness. The image from Fig. 5 b) and c) was low-pass filtered in order to suppress the residual high-frequency noise

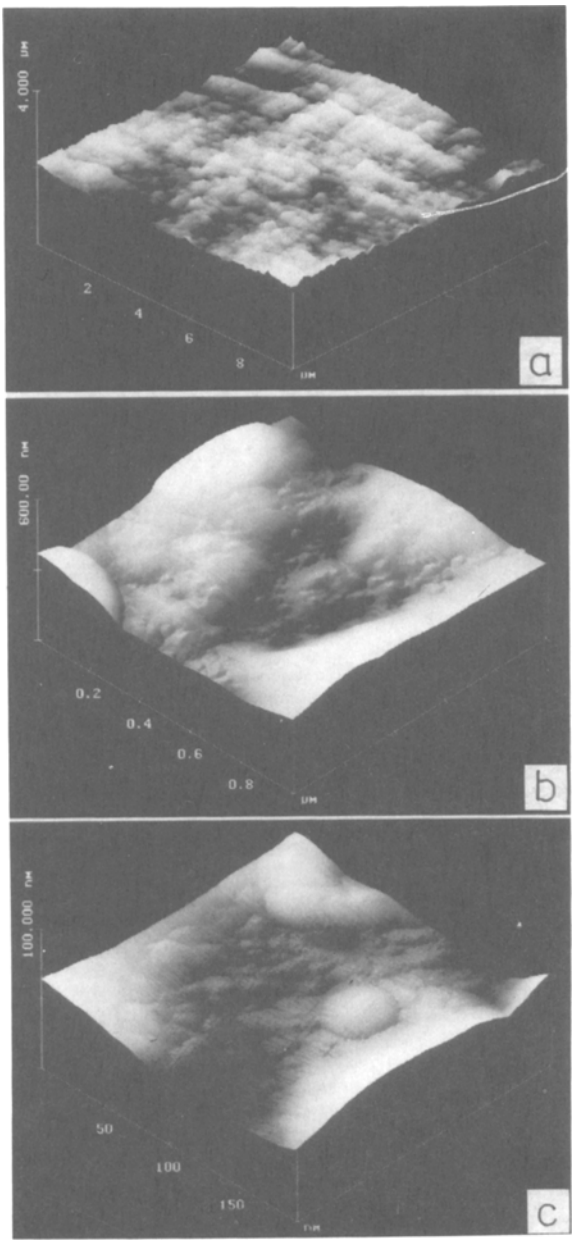


**Fig. 6** 3-D renditions of tapping-mode AFM topographs of the surface of PP/PS(C) exposed by brittle fracture at liquid nitrogen temperature. Scan ranges: a) 10 μm×10 μm; b) 1 μm ×1 μm; c) 200 nm×200 nm. Vertical scale coding: a) – grey scale; b) and c) artificial illumination. The images shown in Fig. 6 b) and c) were low-pass filtered in order to suppress the residual high-frequency noise

posed surfaces through plastic deformation during microtoming at room temperature. However, the extent of this reorganization – reflecting susceptibility to plastic deformation – correlated with the composition of studied materials.

Surfaces of plain PP exposed by microtoming were totally reorganized by deformation – Figs 7a–b. Narrowly-spaced parallel lines seen in these figures are the artifacts created by the irregularities of the cutting edge of the microtome knife (their direction corresponds to the cutting direction). The origin of the semi-periodic undulations perpendicular to the cutting direction is most likely similar to that of so-called Schallamach waves – semi-periodic patterns associated with friction and wear phenomena [12].

Surfaces of PP/PS-M exhibited additionally large holes formed when much harder spherical PS inclusions were torn-out 'plowed' by the knife through the relatively soft PP matrix (Figs 8a, b).

Samples containing highly-dispersed, *in situ* polymerized PS underwent the least extensive reorganization during microtoming. As illustrated in Fig. 9 the features corresponding to internal organization of the spherulites can be still

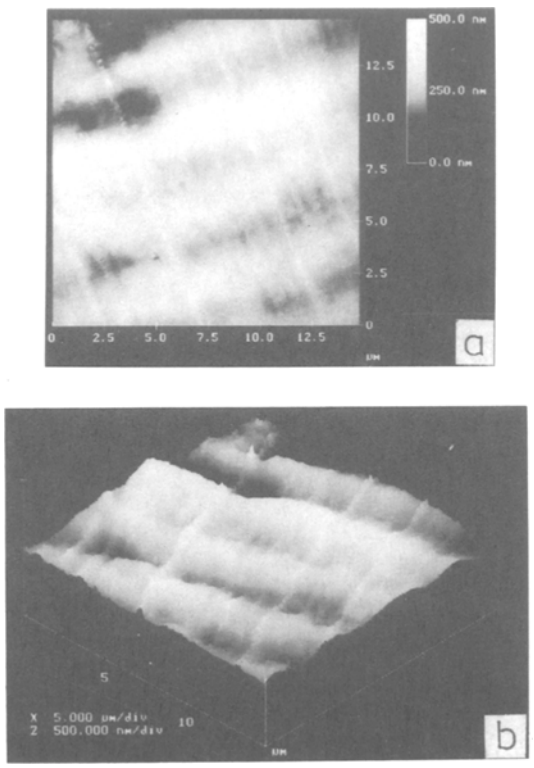


**Fig. 7** Tapping-mode AFM topograph of the microtomed surface of plain PP sample: a) top-view; b) 3-D rendition. Vertical scale coding – gray scale (see insert in Fig. 7a)

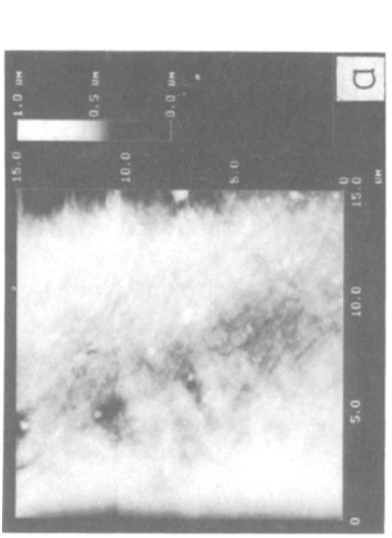


**Fig. 9** Tapping-mode AFM topograph of the microtomed surface of the PP/PS(L) sample: a) top-view; b) 3-D rendition. Vertical scale coding - gray scale (see insert in Fig. 9a)

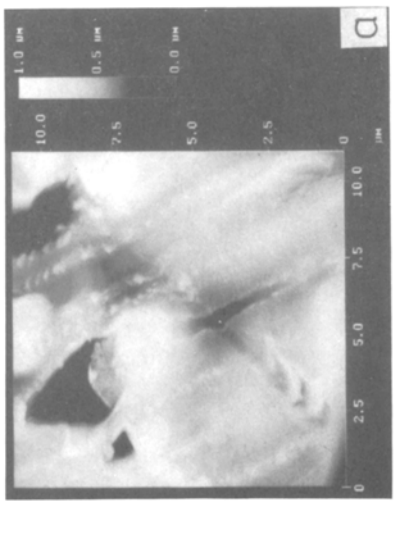


**Fig. 8** Tapping-mode AFM topograph of the microtomed surface of the PP/PS-M sample: a) top-view; b) 3-D rendition. Vertical scale coding - gray scale (see insert in Fig. 8a)

distinguished. This indicates that in contrast with micro-dispersed phase (PP/PS-M), nano-dispersed polystyrene acts as a reinforcing/hardening agent and prevents reorganization of PP matrix through plastic deformation during microtoming.

### *Dynamic mechanical studies*

Figure 10 presents the temperature dependencies of the storage modulus $G'$ and mechanical loss (tan δ) of the polypropylene/polystyrene systems and, for comparison, of plain PP. The plain sample exhibits three maxima on the tan δ curve which are attributed to the following relaxation processes: γ (around 220 K), β (around 277 K) and α (above 300 K with maximum at 340 K). Analysis of the origin of these processes was the subject of numerous studies [e.g. 13–18]. The γ process has been assigned to the local mode relaxation in the amorphous phase. The $G'$ modulus exhibits the plateau at temperature region of the γ process. The β relaxation process is clearly related to the glass – rubber transition of the amorphous phase and is accompanied by a distinct decrease of the $G'$ modulus with the increase of temperature. The nature of the α process is still controversial, however there is a general agreement that it requires the presence of the crystalline phase and occurs in the regions where interlamellar shear is the predominant form of mechanical deformation. The process presumably involves such phenomena $G'$as the intracrystalline relaxations and sliding of tie molecules inside the crystalline blocks. The $G'$ modulus decreases gradually with the increase of temperature in the α relaxation region.

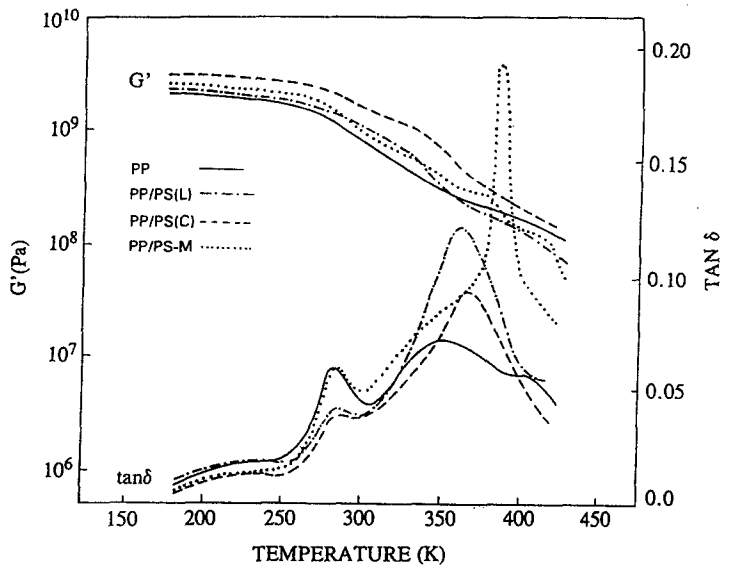


**Fig. 10** Log$G'$ and tan δ dependencies of the individual samples as a function of temperature

It is known that the $G'$ and tan δ spectra are sensitive to PP morphology and the degree of crystallinity. Generally, the intensities of the processes decrease with an increase of the sizes of the spherulites and of the degree of crystallinity [e.g. 18]. In the case considered here one can assume that the plain PP and PP components in the polypropylene/polystyrene systems exhibit a similar morphology, with comparable spherulite dimensions. Therefore the differences in the dynamic mechanical response for the studied polypropylene/polystyrene systems should be ascribed to variations in the phase structure and crystalline perfection of the PP component.

As follows from Fig. 10, in the temperature range below the glass-rubber transition temperature for the PS components, $T_g^{PS}$, the values of $G'$ modulus of PP/PS(L) and PP/PS-M systems are larger than those observed for the plain PP sample. On the contrary – above $T_g^{PS}$ the values of $G'$ for both systems drop below the value of $G'$ observed for the plain PP sample. This behavior indicates that, while in the rubbery phase, the dispersed PS plasticizes the PP matrix of the PP/PS(L) and PP/PS-M systems. Such plasticizing action is not observed however with the PP/PS(C) sample. Over the whole range of temperature its $G'$ values exceed those of the other systems. Since the crystallinities of the PP phase in the PP/PS(L) and PP/PS(C) systems are comparable (Table 3), this indicates that the PS(C) component substantially reinforces the PP matrix and contributes to the transmission of stresses induced during periodic deformation of the system more effectively than uncrosslinked PS(L). Such behavior suggests that the polymer chains of crosslinked PS are more extensively entangled with the PP matrix. In addition, the chemical crosslinks suppress the rubbery flow and liquid flow of the PS(C) phase above $T_g^{PS}$ [19].

The differences of the phase structure of these systems are also reflected in the values of the mechanical loss (tan δ). The largest differences in the tan δ spectra are observed in the temperature region corresponding to the β and α relaxation processes of the PP phase. The presence of the *in situ* polymerized PS component leads to the decrease of the intensity of the β process of PP in two–component systems in comparison with plain PP. This decrease is much more pronounced in the case of PP/PS(C) system. The intensity of the β process in PP/PS-M sample remain similar to that observed for the plain PP sample. Since the PS contents in these systems are similar, the decrease of the β peak intensity most likely reflects the decrease of the molecular mobility of the amorphous phase of PP in the presence of rigid polystyrene formed by polymerization *in situ*. This effect is more pronounced when the dispersed phase is crosslinked, which suggests that physical entanglements between PS and PP chains play some role in immobilization of the amorphous phase of PP.

The α relaxation process for the PP occurs over a broad temperature range, partially overlapping with the temperature range of the glass-rubber transition of PS. For the temperatures at which the polystyrene remains glassy (i.e. at the low range of the α process region) the mechanical loss is decreased only for the

PP/PS(C) system, while for the PP/PS(L) and plain PP samples it is comparable. Since the mechanical loss of glassy polystyrene is only slightly temperature dependent and is considerably smaller than the mechanical loss of PP, we propose that the observed relation reflects the fact that the interlamellar regions of the PP matrix become more rigid in the presence of PS(C) than in the presence of PS(L). As no decrease of the $\alpha$ process intensity is observed for the PP/PS(L) system, one can surmise that the linear component (PS(L)) is only weakly entangled with the PP matrix, and/or its concentration within the interlamellar regions is lower than for the crosslinked counterpart in the PP/PS(C) system. A similar suggestion was made based on the observations by light microscopy. In the case of the PP/PS-M system, which shows poor adhesion between the constituents, a steady enhancement of the tan $\delta$ in relation to the PP sample is observed (293–340 K). This most likely reflects the dominating contribution of the shearing processes generated within the boundary regions between two polymers.

Analysis of the tan $\delta$ maxima, appearing at higher temperatures, provides complementary information. For the polypropylene/polystyrene systems these maxima are shifted towards higher temperature in comparison with the maximum corresponding to the $\alpha$ relaxation of plain PP. These shifts are due to the contribution from the glass-rubber transition of the polystyrene components and depend on their dispersion and chemical constitution. Partial overlap of the mechanical losses of both components makes it difficult to evaluate the extent of modification of the high temperature portion of the $\alpha$ relaxation process of PP. Analysis of the contribution of the rubber-like polystyrene components to the mechanical loss of the polypropylene/polystyrene systems leads to the following conclusions:

– The height of the resultant tan $\delta$ maximum is related not only to the overall polystyrene contents in the PP matrix (Table 1) but also to the volume fraction of the separated domains.

– The higher dispersion of the polystyrene phase and more effective entanglement between both components lead to the broadening of the relaxation peak and to the decrease of its height (successive samples PP/PS-M→PP/PS(L) →PP/PS(C)). This feature can be interpreted as a result of variation in the properties of the interface.

– The glass transition of the polystyrene components in the PP matrices is well reflected in the mechanical measurements and its temperature, indicated by the position of the tan $\delta$ maximum, coincides with the value determined for the pure polystyrene materials by DSC.

Summarizing: The dynamic mechanical studies indicate that the viscoelastic properties of the polypropylene/polystyrene systems depend not only on the properties of the individual constituents but are also strongly affected by the dispersion of the minor component and the nature of the interface. Dispersion of the PS component in materials prepared by *in situ* polymerization, leads to the

increase of rigidity of the mobile phase of PP. This effect is stronger when the PS component is chemically crosslinked.

## Conclusions

The presented results show that the degree of dispersion of the immiscible PS component within the PP matrix can be considerably increased when the PS is introduced by polymerization *in situ* instead of blending with the PP in the molten state.

AFM observations of fracture surfaces of polypropylene/polystyrene systems obtained by *in situ* polymerization of the polystyrene only in a few cases revealed the presence of nanometer size domains. Basing on the rare occurrence of such observations we propose that the predominant fraction of polystyrene was highly dispersed within noncrystalline, both inter- and intraspherulitic regions of the PP phase where the ST polymerization occurred. Within those regions both polymer components form entangled regions which substantially modify the interface in these systems. The extent of this modification appeared to be larger when the PS constituent was crosslinked. Therefore, the relaxation processes intensity of the PP phase was more restrained in the PP/PS system containing crosslinked PS.

In the PP/PS-M system prepared by melt blending the dispersed phase was segregated in the form of micron size domains. In contrast with the previously discussed polypropylene/polystyrene systems the PP/PS-M system was characterized by the sharp interphase profile and by poor adhesion between components. For this reason the dynamic mechanical behavior of this system can be explained as a result of simple superposition of mechanical properties of two homopolymers.

* * *

Mechanical measurements were carried out by M.P at the Max-Planck-Institut für Polymerforschung in Mainz (FRG) in Dr. T. Pakula's research group and were made possible by the DAAD Fellowship. T. K. was supported in part by the Office of Naval Research.

## References

1 P. Milczarek, M. Pluta and M. Kryszewski, Acta Polymerica, 40 (1989) 575.
2 M. Pluta, P. Milczarek, A. Włochowicz and M. Kryszewski, Acta Polymerica, 42 (1991) 485.
3 M. Kryszewski, M. Pluta, M. Trznadel and P. Milczarek, Macromol. Chem., Macromol. Symp., 62 (1992) 191.
4 P. Milczarek, M. Pluta and M. Kryszewski, Colloid & Polym. Sci., 267 (1989) 209.
5 M. Pluta, P. Milczarek and M. Kryszewski, Colloid & Polym. Sci., 265 (1987) 490.
6 M. Trznadel, M. Pluta and M. Kryszewski, J. Appl. Polym. Sci., 50 (1993) 637.
7 M. Pluta, P. Milczarek, A. Włochowicz and M. Kryszewski, Acta Polymerica, 42 (1991) 306.
8 Q. Zhong, D. Inniss, K. Kjoller and V. B. Elings, Surface Science, 290 (1993) L688.

9 R. L. Miller, in Encyclopedia of Polymer Science and Technology, H. F. Mark, N. G. Gaylord, and N. M. Bikales, Eds., Wiley-Interscience, New York, 1966, Vol. 4, pp. 448–520.
10 D. Derek, D. Lath and V. Durdovic, J. Polym. Sci., 14 (1967) 659.
11 M. Trznadel, M. Pluta, and M. Kryszewski, J. Appl. Polym. Sci., 49 (1993) 1405.
12 B. W. Cherry, Polymer Surfaces, Cambridge 1981.
13 J. M. Crissman, J. Polym. Sci., Polym. Phys., Part A-2, 7 (1969) 389.
14 M. Takayanagi, M. Yoshino, and S. Minami, J. Polym. Sci., 61 (1962) S7.
15 R. H. Boyd, Polym. Eng. Sci., 19 (1979) 1010.
16 N. G. McCrum, J. Polym. Sci., Part: Polymer Letters, 2 (1964) 495.
17 Y. Wada and Y. Hotta, J. Polym. Sci., C, 23 (1968) 583.
18 M. Pluta and M. Kryszewski, Acta Polymerica, 38 (1987) 42.
19 D. W. Van Krevelen and P. J. Hoftyzer, 'Properties of polymers. Their estimation and correlation with chemical structure'. Eds. Elsevier Scientific Publishing Company, Amsterdam-Oxford-New York 1976, p. 274.